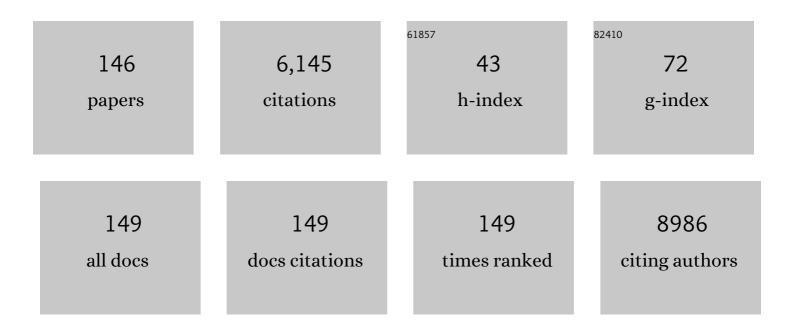
List of Publications by Year in descending order

Source: https://exaly.com/author-pdf/4824177/publications.pdf Version: 2024-02-01



HONCYLI SUN

#	Article	IF	CITATIONS
1	Threeâ€Dimensional Assembly of Single‣ayered MoS ₂ . Advanced Materials, 2014, 26, 964-969.	11.1	415
2	Synthesis of hierarchical flower-like ZnO nanostructures and their functionalization by Au nanoparticles for improved photocatalytic and high performance Li-ion battery anodes. Journal of Materials Chemistry, 2011, 21, 7723.	6.7	369
3	Micro-/Nanostructured Co ₃ O ₄ Anode with Enhanced Rate Capability for Lithium-Ion Batteries. ACS Applied Materials & Interfaces, 2014, 6, 7236-7243.	4.0	214
4	Nitrogen-enriched electrospun porous carbon nanofiber networks as high-performance free-standing electrode materials. Journal of Materials Chemistry A, 2014, 2, 19678-19684.	5.2	165
5	Mesoporous Co3O4 sheets/3D graphene networks nanohybrids for high-performance sodium-ion battery anode. Journal of Power Sources, 2015, 273, 878-884.	4.0	164
6	Solid-State Thin-Film Supercapacitors with Ultrafast Charge/Discharge Based on N-Doped-Carbon-Tubes/Au-Nanoparticles-Doped-MnO ₂ Nanocomposites. Nano Letters, 2016, 16, 40-47.	4.5	159
7	Confined-interface-directed synthesis of Palladium single-atom catalysts on graphene/amorphous carbon. Applied Catalysis B: Environmental, 2018, 225, 291-297.	10.8	159
8	Defect engineering of oxide perovskites for catalysis and energy storage: synthesis of chemistry and materials science. Chemical Society Reviews, 2021, 50, 10116-10211.	18.7	140
9	Core–Shell Ellipsoidal MnCo ₂ O ₄ Anode with Micro-/Nano-Structure and Concentration Gradient for Lithium-Ion Batteries. ACS Applied Materials & Interfaces, 2014, 6, 21325-21334.	4.0	114
10	Pt Nanoparticles Embedded in Colloidal Crystal Template Derived 3D Ordered Macroporous Ce _{0.6} Zr _{0.3} Y _{0.1} O ₂ : Highly Efficient Catalysts for Methane Combustion. ACS Catalysis, 2015, 5, 1781-1793.	5.5	113
11	Mesoporous Co3O4 nanosheets-3D graphene networks hybrid materials for high-performance lithium ion batteries. Electrochimica Acta, 2014, 118, 1-9.	2.6	112
12	Electrical Breakdown of Nanowires. Nano Letters, 2011, 11, 4647-4651.	4.5	107
13	Ordered meso- and macroporous perovskite oxide catalysts for emerging applications. Chemical Communications, 2018, 54, 6484-6502.	2.2	104
14	Electrochemically Seed-Mediated Synthesis of Sub-10 nm Tetrahexahedral Pt Nanocrystals Supported on Graphene with Improved Catalytic Performance. Journal of the American Chemical Society, 2016, 138, 5753-5756.	6.6	99
15	Uniform Fe3O4 microflowers hierarchical structures assembled with porous nanoplates as superior anode materials for lithium-ion batteries. Applied Surface Science, 2016, 389, 240-246.	3.1	96
16	Morphology-controlled synthesis of Co3O4 porous nanostructures for the application as lithium-ion battery electrode. Electrochimica Acta, 2013, 89, 199-205.	2.6	91
17	Three-Dimensionally Ordered Macroporous La _{0.6} Sr _{0.4} MnO ₃ Supported Ag Nanoparticles for the Combustion of Methane. Journal of Physical Chemistry C, 2014, 118, 14913-14928.	1.5	89
18	Porous mesocarbon microbeads with graphitic shells: constructing a high-rate, high-capacity cathode for hybrid supercapacitor. Scientific Reports, 2013, 3, 2477.	1.6	79

#	Article	IF	CITATIONS
19	Well-Constructed Single-Layer Molybdenum Disulfide Nanorose Cross-Linked by Three Dimensional-Reduced Graphene Oxide Network for Superior Water Splitting and Lithium Storage Property. Scientific Reports, 2015, 5, 8722.	1.6	79
20	Simultaneous modulation of surface composition, oxygen vacancies and assembly in hierarchical Co ₃ O ₄ mesoporous nanostructures for lithium storage and electrocatalytic oxygen evolution. Nanoscale, 2017, 9, 14431-14441.	2.8	77
21	Morphology-controlled synthesis of ZnO 3D hierarchical structures and their photocatalytic performance. CrystEngComm, 2012, 14, 8626.	1.3	75
22	Enhanced Photoluminescence and Field-Emission Behavior of Vertically Well Aligned Arrays of In-Doped ZnO Nanowires. ACS Applied Materials & Interfaces, 2011, 3, 1299-1305.	4.0	72
23	SnS2 nanoflakes decorated multiwalled carbon nanotubes as high performance anode materials for lithium-ion batteries. Materials Research Bulletin, 2014, 49, 319-324.	2.7	69
24	Co ₉ S ₈ nanoparticles encapsulated in nitrogen-doped mesoporous carbon networks with improved lithium storage properties. RSC Advances, 2016, 6, 31775-31781.	1.7	69
25	Three-Dimensional ZnO Hierarchical Nanostructures: Solution Phase Synthesis and Applications. Materials, 2017, 10, 1304.	1.3	69
26	Nanoparticle Decorated Ultrathin Porous Nanosheets as Hierarchical Co3O4 Nanostructures for Lithium Ion Battery Anode Materials. Scientific Reports, 2016, 6, 20592.	1.6	68
27	Recovery of lithium from the effluent obtained in the process of spent lithium-ion batteries recycling. Journal of Environmental Management, 2017, 198, 84-89.	3.8	67
28	Lead-free double halide perovskite Cs ₃ BiBr ₆ with well-defined crystal structure and high thermal stability for optoelectronics. Journal of Materials Chemistry C, 2019, 7, 3369-3374.	2.7	66
29	Meso-Molding Three-Dimensional Macroporous Perovskites: A New Approach to Generate High-Performance Nanohybrid Catalysts. ACS Applied Materials & Interfaces, 2016, 8, 2457-2463.	4.0	64
30	Porous Co3O4@CoO composite nanosheets as improved anodes for lithium-ion batteries. Journal of Alloys and Compounds, 2020, 834, 155030.	2.8	61
31	Polyoxometalate Clusterâ€Incorporated Metalâ€Organic Framework Hierarchical Nanotubes. Small, 2016, 12, 2982-2990.	5.2	60
32	Noble metal nanoparticle-functionalized ZnO nanoflowers for photocatalytic degradation of RhB dye and electrochemical sensing of hydrogen peroxide. Journal of Nanoparticle Research, 2016, 18, 1.	0.8	59
33	Three-dimensional iron sulfide-carbon interlocked graphene composites for high-performance sodium-ion storage. Nanoscale, 2018, 10, 7851-7859.	2.8	56
34	Fe3O4@polyaniline yolk-shell micro/nanospheres as bifunctional materials for lithium storage and electromagnetic wave absorption. Applied Surface Science, 2018, 427, 1054-1063.	3.1	55
35	Enhanced photocatalytic and electrochemical properties of Au nanoparticles supported TiO2 microspheres. New Journal of Chemistry, 2014, 38, 1424.	1.4	52
36	Porous polyhedral and fusiform Co3O4 anode materials for high-performance lithium-ion batteries. Electrochimica Acta, 2014, 135, 420-427.	2.6	52

#	Article	IF	CITATIONS
37	SnO2/ZnO composite structure for the lithium-ion battery electrode. Journal of Solid State Chemistry, 2012, 196, 326-331.	1.4	51
38	New spinel high-entropy oxides (FeCoNiCrMnXLi)3O4 (X = Cu, Mg, Zn) as the anode material for lithium-ion batteries. Ceramics International, 2021, 47, 32025-32032.	2.3	50
39	Facile synthesis of single-crystal mesoporous CoNiO2 nanosheets assembled flowers as anode materials for lithium-ion batteries. Electrochimica Acta, 2014, 132, 404-409.	2.6	48
40	Polyaniline coated Fe ₃ O ₄ hollow nanospheres as anode materials for lithium ion batteries. Sustainable Energy and Fuels, 2017, 1, 915-922.	2.5	48
41	3D anatase TiO2 hollow microspheres assembled with high-energy {001} facets for lithium-ion batteries. RSC Advances, 2012, 2, 7901.	1.7	47
42	Phosphate tuned copper electrodeposition and promoted formic acid selectivity for carbon dioxide reduction. Journal of Materials Chemistry A, 2017, 5, 11905-11916.	5.2	46
43	Continuous flow reduction of organic dyes over Pd-Fe alloy based fibrous catalyst in a fixed-bed system. Chemical Engineering Science, 2021, 231, 116303.	1.9	45
44	3D network single-phase Ni0.9Zn0.1O as anode materials for lithium-ion batteries. Nano Energy, 2016, 28, 338-345.	8.2	43
45	Magnetically Actuated Wormlike Nanomotors for Controlled Cargo Release. ACS Applied Materials & Interfaces, 2015, 7, 26017-26021.	4.0	42
46	Micro-spherical CoCO3 anode for lithium-ion batteries. Materials Letters, 2014, 131, 236-239.	1.3	41
47	Improved lithium storage properties of Co3O4 nanoparticles via laser irradiation treatment. Electrochimica Acta, 2018, 281, 31-38.	2.6	41
48	Electronic structure modulation with ultrafine Fe3O4 nanoparticles on 2D Ni-based metal-organic framework layers for enhanced oxygen evolution reaction. Journal of Energy Chemistry, 2022, 65, 78-88.	7.1	41
49	Unhindered Brownian Motion of Individual Nanoparticles in Liquid-Phase Scanning Transmission Electron Microscopy. Nano Letters, 2020, 20, 7108-7115.	4.5	40
50	Substrate-Assisted Encapsulation of Pd-Fe Bimetal Nanoparticles on Functionalized Silica Nanotubes for Catalytic Hydrogenation of Nitroarenes and Azo Dyes. ACS Applied Nano Materials, 2021, 4, 5854-5863.	2.4	39
51	A sandwich structure of mesoporous anatase TiO ₂ sheets and reduced graphene oxide and its application as lithium-ion battery electrodes. RSC Advances, 2014, 4, 43039-43046.	1.7	38
52	Defective ZnCo2O4 with Zn vacancies: Synthesis, property and electrochemical application. Journal of Alloys and Compounds, 2017, 724, 1149-1156.	2.8	34
53	Electron inelastic mean free path in water. Nanoscale, 2020, 12, 20649-20657.	2.8	34
54	The control of the growth orientations of electrodeposited single-crystal nanowire arrays: a case study for hexagonal CdS. Nanotechnology, 2008, 19, 225601.	1.3	33

#	Article	IF	CITATIONS
55	Synthesis of porous MnCo ₂ O ₄ microspheres with yolk–shell structure induced by concentration gradient and the effect on their performance in electrochemical energy storage. RSC Advances, 2016, 6, 10763-10774.	1.7	33
56	Preparation and electrochemical properties of mesoporous NiCo2O4 double-hemisphere used as anode for lithium-ion battery. Journal of Colloid and Interface Science, 2018, 529, 357-365.	5.0	33
57	Enhanced high-frequency microwave absorption of Fe3O4 architectures based on porous nanoflake. Ceramics International, 2017, 43, 16013-16017.	2.3	32
58	Engineering Surface Structure and Defect Chemistry of Nanoscale Cubic Co ₃ O ₄ Crystallites for Enhanced Lithium and Sodium Storage. ACS Applied Nano Materials, 2020, 3, 3892-3903.	2.4	32
59	Mean Inner Potential of Liquid Water. Physical Review Letters, 2020, 124, 065502.	2.9	32
60	Recent advances of metal telluride anodes for high-performance lithium/sodium–ion batteries. Materials Horizons, 2022, 9, 524-546.	6.4	32
61	Atomic ordering kinetics of FePt thin films: Nucleation and growth of L10 ordered domains. Journal of Applied Physics, 2007, 101, 093911.	1.1	31
62	Enhancement of the coercivity of electrodeposited nickel nanowire arrays. Materials Letters, 2007, 61, 1859-1862.	1.3	31
63	Hierarchically porous indium oxide nanolamellas with ten-parts-per-billion-level formaldehyde-sensing performance. Sensors and Actuators B: Chemical, 2015, 206, 714-720.	4.0	31
64	Engineering the Surface/Interface Structures of Titanium Dioxide Micro and Nano Architectures towards Environmental and Electrochemical Applications. Nanomaterials, 2017, 7, 382.	1.9	31
65	Nanosized high entropy spinel oxide (FeCoNiCrMn) ₃ O ₄ as a highly active and ultra-stable electrocatalyst for the oxygen evolution reaction. Sustainable Energy and Fuels, 2022, 6, 1479-1488.	2.5	31
66	In-situ synthesis of niobium-doped TiO2 nanosheet arrays on double transition metal MXene (TiNbCTx) as stable anode material for lithium-ion batteries. Journal of Colloid and Interface Science, 2022, 617, 147-155.	5.0	31
67	Tuning lithium storage properties of cubic Co3O4 crystallites: The effect of oxygen vacancies. Journal of Alloys and Compounds, 2019, 787, 720-727.	2.8	30
68	Recent advances of Li7La3Zr2O12-based solid-state lithium batteries towards high energy density. Energy Storage Materials, 2022, 49, 299-338.	9.5	30
69	Hierarchical CoNiO ₂ structures assembled from mesoporous nanosheets with tunable porosity and their application as lithium-ion battery electrodes. New Journal of Chemistry, 2014, 38, 3084-3091.	1.4	29
70	Ag TiO 2 nanocomposite for environmental and sensing applications. Materials Chemistry and Physics, 2016, 181, 194-203.	2.0	29
71	Ultrahigh capacitive performance of three-dimensional electrode nanomaterials based on α-MnO2 nanocrystallines induced by doping Au through Ãscale channels. Nano Energy, 2016, 21, 39-50.	8.2	29
72	<i>In situ</i> electrochemistry inside a TEM with controlled mass transport. Nanoscale, 2020, 12, 22192-22201.	2.8	29

#	Article	IF	CITATIONS
73	Boosting electrochemical reaction and suppressing phase transition with a high-entropy O3-type layered oxide for sodium-ion batteries. Journal of Materials Chemistry A, 2022, 10, 14943-14953.	5.2	29
74	Enhanced Catalytic Efficiency of Pt Nanoparticles Supported on 3D Ordered Macro″Mesoporous Ce _{0.6} Zr _{0.3} Y _{0.1} O ₂ for Methane Combustion. Small, 2015, 11, 2366-2371.	5.2	26
75	Formation of graphene-like 2D spinel MnCo2O4 and its lithium storage properties. Journal of Alloys and Compounds, 2017, 695, 2937-2944.	2.8	26
76	Chemical reduction-induced oxygen deficiency in Co3O4 nanocubes as advanced anodes for lithium ion batteries. Solid State Ionics, 2019, 334, 117-124.	1.3	25
77	Chemical activation of hollow carbon nanospheres induced self-assembly of metallic 1T phase MoS2 ultrathin nanosheets for electrochemical lithium storage. Electrochimica Acta, 2020, 353, 136545.	2.6	25
78	Nanoscale niobium oxides anode for electrochemical lithium and sodium storage: a review of recent improvements. Journal of Nanostructure in Chemistry, 2021, 11, 33-68.	5.3	25
79	Constructing aligned γ-Fe ₂ O ₃ nanorods with internal void space anchored on reduced graphene oxide nanosheets for excellent lithium storage. RSC Advances, 2015, 5, 91574-91580.	1.7	24
80	Pressure-induced preferential growth of nanocrystals in amorphous Nd ₉ Fe ₈₅ B ₆ . Nanotechnology, 2008, 19, 285603.	1.3	23
81	Controllable growth of electrodeposited single-crystal nanowire arrays: The examples of metal Ni and semiconductor ZnS. Journal of Crystal Growth, 2007, 307, 472-476.	0.7	22
82	Ag-Modified In2O3/ZnO Nanobundles with High Formaldehyde Gas-Sensing Performance. Sensors, 2015, 15, 20086-20096.	2.1	22
83	Pressure-induced transition-temperature reduction in ZnS nanoparticles. Nanotechnology, 2008, 19, 095704.	1.3	21
84	Free-standing Ni-Co alloy nanowire arrays: Efficient and robust catalysts toward urea electro-oxidation. Electrochimica Acta, 2018, 283, 1277-1283.	2.6	21
85	High-performance lithium storage based on the synergy of atomic-thickness nanosheets of TiO2(B) and ultrafine Co3O4 nanoparticles. Journal of Power Sources, 2017, 363, 110-116.	4.0	20
86	Low-temperature synthesis of wurtzite ZnS single-crystal nanowire arrays. Nanotechnology, 2007, 18, 115604.	1.3	19
87	Facile synthesis of Co3O4 mesoporous nanosheets and their lithium storage properties. Materials Letters, 2014, 125, 103-106.	1.3	18
88	Microwave assisted crystalline and morphology evolution of flower-like Fe2O3@ iron doped K-birnessite composite and its application for lithium ion storage. Applied Surface Science, 2020, 525, 146513.	3.1	18
89	Microstructure and magnetic behavior of electrodeposited CoPt thick films upon annealing. Materials Letters, 2008, 62, 309-312.	1.3	17
90	Low-voltage magnetoresistance in silicon. Nature, 2013, 501, E1-E1.	13.7	16

6

#	Article	IF	CITATIONS
91	Fine control over the morphology and photocatalytic activity of 3D ZnO hierarchical nanostructures: capping vs. etching. RSC Advances, 2015, 5, 56232-56238.	1.7	16
92	Enhanced field emission of ZnO nanoneedle arrays via solution etching at room temperature. Materials Letters, 2017, 206, 162-165.	1.3	16
93	Au nanoparticles decorated CuO nanowire arrays with enhanced photocatalytic properties. Materials Letters, 2013, 108, 41-45.	1.3	15
94	Oxygen vacancies enhance lithium storage performance in ultralong vanadium pentoxide nanobelt cathodes. Journal of Colloid and Interface Science, 2019, 539, 118-125.	5.0	15
95	Nanoscale Phase Engineering in Two-Dimensional Niobium Pentoxide Anodes toward Excellent Electrochemical Lithium Storage. ACS Applied Energy Materials, 2021, 4, 4551-4560.	2.5	15
96	Diameter- and current-density-dependent growth orientation of hexagonal CdSe nanowire arrays via electrodeposition. Nanotechnology, 2009, 20, 425603.	1.3	14
97	Optimizing oxygen vacancies can improve the lithium storage properties in NiO porous nanosheet anodes. Materials Characterization, 2020, 166, 110447.	1.9	14
98	Crystalline Planes templated engineering of defect chemistry in Cobalt(II, III) oxide anodes for lithium ion batteries. Journal of Alloys and Compounds, 2021, 850, 156858.	2.8	14
99	Hydrazine hydrate reduction-induced oxygen vacancy formation in Co3O4 porous nanosheets to optimize the electrochemical lithium storage. Journal of Alloys and Compounds, 2021, 861, 157994.	2.8	14
100	Development of Silver Nanowires Based Highly Sensitive Amperometric Glucose Biosensor. Electroanalysis, 2015, 27, 1498-1506.	1.5	13
101	Tuning the phase composition in polymorphic Nb2O5 nanoplates for rapid and stable lithium ion storage. Electrochimica Acta, 2021, 399, 139368.	2.6	13
102	Covalent Pinning of Highly Dispersed Ultrathin Metallic-Phase Molybdenum Disulfide Nanosheets on the Inner Surface of Mesoporous Carbon Spheres for Durable and Rapid Sodium Storage. ACS Applied Materials & Interfaces, 2021, 13, 58652-58664.	4.0	13
103	Nucleation and growth processes of α-Fe nanocrystals in amorphous NdFeBCoDy: In situ x-ray diffraction studies. Applied Physics Letters, 2005, 86, 092501.	1.5	12
104	Silicon-Encapsulated Hollow Carbon Nanofiber Networks as Binder-Free Anodes for Lithium Ion Battery. Journal of Nanomaterials, 2014, 2014, 1-10.	1.5	12
105	Hierarchical nanoflowers assembled with Au nanoparticles decorated ZnO nanosheets toward enhanced photocatalytic properties. Materials Letters, 2017, 190, 185-187.	1.3	12
106	In Situ Production of Graphene–Fiber Hybrid Structures. ACS Applied Materials & Interfaces, 2017, 9, 25474-25480.	4.0	12
107	Orientation Growth and Magnetic Properties of Electrochemical Deposited Nickel Nanowire Arrays. Catalysts, 2019, 9, 152.	1.6	12
108	Synthesis of ZnS hollow nanoneedles via the nanoscale Kirkendall effect. Journal of Nanoparticle Research, 2011, 13, 97-103.	0.8	11

#	Article	IF	CITATIONS
109	Confined Growth of ZIFâ€8 Nanocrystals with Tunable Structural Colors. Advanced Materials Interfaces, 2018, 5, 1701270.	1.9	11
110	Highly Ordered 3D Silicon Microâ€Mesh Structures Integrated with Nanowire Arrays: A Multifunctional Platform for Photodegradation, Photocurrent Generation, and Materials Conversion. ChemNanoMat, 2019, 5, 92-100.	1.5	11
111	Ultrathin Metallic-Phase Molybdenum Disulfide Nanosheets Stabilized on Functionalized Carbon Nanotubes Via Covalent Interface Interaction for Sodium- and Lithium-Ion Storage. ACS Applied Energy Materials, 2021, 4, 9440-9449.	2.5	11
112	Enhanced coercivity in α-(Fe,Co)/(Nd,Pr) ₂ Fe ₁₄ B nanocomposite magnets via interfacial modification. Journal Physics D: Applied Physics, 2008, 41, 155003.	1.3	10
113	Fabrication and temperature dependent magnetic properties of Ni–Cu–Co composite nanowires. Physica B: Condensed Matter, 2015, 475, 99-104.	1.3	10
114	Engineering the surface of rutile TiO ₂ nanoparticles with quantum pits towards excellent lithium storage. RSC Advances, 2016, 6, 66197-66203.	1.7	10
115	Ultrafast and Stable Lithium Storage Enabled by the Electric Field Effect in Layer-Structured Tablet-Like NH ₄ TiOF ₃ Mesocrystals. ACS Applied Materials & Interfaces, 2020, 12, 20404-20413.	4.0	10
116	<i>L</i> 1 ₀ phase transition in FePt thin films via direct interface reaction. Journal Physics D: Applied Physics, 2008, 41, 235001.	1.3	9
117	Nucleation-promotedL10ordering in FePt thin films with ultrasmall grain size. Journal Physics D: Applied Physics, 2008, 41, 135009.	1.3	9
118	One-pot hydrothermal synthesis of hollow Fe3O4 microspheres assembled with nanoparticles for lithium-ion battery anodes. Materials Letters, 2016, 172, 76-80.	1.3	9
119	Boosting the electrocatalytic hydrogen evolution and sodium-storage properties of Co ₉ S ₈ nanoparticles <i>via</i> encapsulation with nitrogen-doped few-layer graphene networks. Sustainable Energy and Fuels, 2021, 5, 4618-4627.	2.5	9
120	Synthesis and characterization of multiwalled carbon nanotube/CdS core/shell heterostructures. Solid State Communications, 2010, 150, 820-823.	0.9	8
121	Space onfined Creation of Nanoframes In Situ on Reduced Graphene Oxide. Small, 2015, 11, 1512-1518.	5.2	7
122	Electrical transport properties of single crystal vanadium pentoxide nanowires. Materials Chemistry and Physics, 2015, 159, 19-24.	2.0	7
123	Lower-voltage plateau Zn-substituted Co3O4 submicron spheres anode for Li-ion half and full batteries. Journal of Alloys and Compounds, 2022, 890, 161888.	2.8	7
124	Interface reaction-accelerated L10 ordering of FePt thin films. Scripta Materialia, 2007, 57, 77-80.	2.6	6
125	Activation volume for nanocrystal growth in amorphous Nd9Fe85B6. Journal of Applied Physics, 2008, 104, 086103.	1.1	6
126	Enhanced conductivity of magnetorheological fluids based on silver coated carbonyl particles. Journal of Materials Science: Materials in Electronics, 2016, 27, 255-259.	1.1	6

#	Article	IF	CITATIONS
127	Self-assembly of flower-like LaNiAlO3-supported nickel catalysts for CO methanation. Catalysis Communications, 2018, 115, 40-44.	1.6	6
128	Frequency stable dielectric constant with reduced dielectric loss of one-dimensional ZnO–ZnS heterostructures. Nanoscale, 2021, 13, 15711-15720.	2.8	6
129	Initiation and Progression of Anisotropic Galvanic Replacement Reactions in a Single Ag Nanowire: Implications for Nanostructure Synthesis. ACS Applied Nano Materials, 2021, 4, 12346-12355.	2.4	6
130	Shape-controlled synthesis of metal nanocrystals–multiwalled carbon nanotubes hybrid structures via electrodeposition. Materials Letters, 2011, 65, 3482-3485.	1.3	5
131	Graphene Oxide-Directed Tunable Assembly of MoS2 Ultrathin Nanosheets for Electrocatalytic Hydrogen Evolution. ChemistrySelect, 2017, 2, 4696-4704.	0.7	5
132	Oxygen-deficient polymorphic Nb2O5 micro/nanoscale three-dimensionally interconnected anodes with enhanced rate capability for lithium storage. Journal of Alloys and Compounds, 2022, 911, 165064.	2.8	5
133	Hierarchical ultrathin rolled-up Co(OH)(CO3)0.5films assembled on Ni0.25Co0.75Sxnanosheets for enhanced supercapacitive performance. RSC Advances, 2014, 4, 57458-57462.	1.7	4
134	Optical and photocatalytic properties of indium phosphide nanoneedles and nanotubes. Materials Science in Semiconductor Processing, 2017, 68, 270-274.	1.9	4
135	MWCNT synergy for boosting the electrochemical kinetics of V ₂ O ₅ cathode for lithium-ion batteries. New Journal of Chemistry, 2022, 46, 3417-3425.	1.4	4
136	Solvothermal synthesis and structure of InP single-crystal nanoneedles and nanotubes. Materials Letters, 2014, 129, 31-34.	1.3	3
137	High-Throughput Wafer-Scale Wrinkle Patterning: a Single-Step Fabrication Process and Applications for Tunable Optical Transmittance. ACS Applied Electronic Materials, 2021, 3, 3200-3206.	2.0	3
138	Graphene Oxide Functionalized with Silver Nanoparticles and ZnO Synergic Nanocomposite as an Efficient Electrochemical Sensor for Diclofenac Sodium. Nano, 2021, 16, .	0.5	3
139	Catalysis: Enhanced Catalytic Efficiency of Pt Nanoparticles Supported on 3D Ordered Macro-/Mesoporous Ce0.6Zr0.3Y0.1O2for Methane Combustion (Small 20/2015). Small, 2015, 11, 2365-2365.	5.2	2
140	Assembly of multicomponent nanoframes via the synergistic actions of graphene oxide space confinement effect and oriented cation exchange. Nanotechnology, 2015, 26, 445601.	1.3	2
141	CoP Nanoparticles Fabricated Through the Nanoscale Kirkendall Effect Immobilized in 3D Hollow Carbon Frameworks for Oxygen Evolution Reaction. Journal of the Electrochemical Society, 2021, 168, 094501.	1.3	2
142	Atomic Ordering Kinetics of FePt Thin Films. Journal of Nanoscience and Nanotechnology, 2009, 9, 1141-1143.	0.9	1
143	Thermal Expansion Behavior of Hexagonal ZnS Single-Crystal Nanowires Embedded in Anodized Aluminum Oxide Template. Chinese Physics Letters, 2010, 27, 106201.	1.3	1
144	Preparation and magnetic properties of cylindrical permalloy nanowire arrays. MRS Communications, 0, , 1.	0.8	1

#	Article	IF	CITATIONS
145	Ultrathin metallic phase MoS2 nanosheets decorated hollow carbon spheres for sodium and potassium ions storage. Solid State Ionics, 2022, 375, 115853.	1.3	1
146	Plasma-Assisted Microcontact Printing. ACS Applied Materials & amp; Interfaces, 2022, , .	4.0	0